LA-UR-19-30451
Approved for public release; distribution is unlimited.

Title: Uncertainty in an Equation of State: How Tightly do Data Constrain Quantities of Interest?

Author(s): Fraser, Andrew Mcleod
Andrews, Stephen Arthur

Intended for: Report

Issued: 2019-10-15 (Draft)

Uncertainty in an Equation of State: How Tightly do Data Constrain Quantities of Interest?

Andrew Fraser and Stephen Andrews

Abstract

We illustrate two applications of F_UNCLE analysis using the associated software and data from several experiments with PBX-9501. In the first application, we investigate the consistency of *out of sample* experimental data with physical principles and data used for calibration. In the second application, we calculate the risk that the value of a cost function (often called a *metric*) exceeds a threshold.

1 Introduction

In previous work[1, 2] we described a procedure for fitting unknown functions to experimental data subject to constraints. We called the procedure *Functional Uncertainty Constrained by Law and Experiment* or F_UNCLE. In [3] we reported applying F_UNCLE to data from four kinds of experiments [4, 5, 6, 7, 8] to obtain both an estimate of the EOS for the gasses produced by detonating PBX-9501 and an estimate of the corresponding uncertainty. Here we demonstrate the application of those results to two questions about an experiment not used for the estimation, namely: Is the uncertainty in the EOS large enough to permit an EOS that would let a simulation match the data? And is the risk of the value of a specific cost function or metric exceeding a specified threshold acceptable?

1.1 Definitions

We begin by defining the following quantities and functions:

V_{measured}**:** An experimentally measured velocity as a function of time. The trace is from probe 5 of shot 3 of the experiments by Pemberton et al.[6]. While other traces from that set of experiments were used to estimate the EOS, probe 5 of shot 3 was not among them.

μ_{MAP}**:** The nominal (maximum a posterior probability) vector of degrees of freedom.

V_{nominal}**:** The velocity simulated using μ_{MAP}.

$\mathcal{E}$: The difference between a simulation and a measured PDV trace:

$$\mathcal{E}(t) \equiv V_{\text{nominal}} - V_{\text{measured}} \tag{1}$$

$\mathbf{P_{S,CJ(\rho)}}$: A model of the HE products EOS:

$$P_{S,CJ(\rho)} \equiv \text{Pressure as a function of density on the CJ isentrope} \tag{2}$$

$\mathbf{u_{P_{S,CJ(\rho)}}}$: The uncertainty

$$u_{P_{S,CJ(\rho)}} \equiv \text{uncertainty in a model of the HE products EOS} \tag{3}$$

ϵ: A deviation from nominal:

$$\epsilon(t) = V(t) - V_{\text{nominal}}(t)$$

$\mathcal{C}$: A cost functional:

$$\mathcal{C}(\epsilon) \equiv \langle \epsilon, V_{\text{cost}} \rangle \tag{4}$$

$\mathbf{V}_{\text{cost}}$: In (4), the function V_{cost} is a test direction and its magnitude defines the maximum acceptable cost.

$\mathcal{C}_{\text{limit}}$: The maximum acceptable cost

$$\begin{aligned} \mathcal{C}_{\text{limit}} &= \langle V_{\text{cost}}, V_{\text{cost}} \rangle \\ &= 0.01384 \end{aligned}$$

Characteristics of the EOS, $P_{S,CJ(\rho)}$, velocity traces, and the cost function appear in Fig. 1.

Now we pose our questions using the above notation:

Q1: Is the uncertainty $u_{P_{S,CJ(\rho)}}$ large enough to allow a pressure, $\mathcal{P}_1$, that would explain $\mathcal{E}$?

Q2: Is the uncertainty $u_{P_{S,CJ(\rho)}}$ small enough to ensure that P_{risk}, the probability of a cost greater than $\mathcal{C}(V_{\text{cost}})$, is less than a specified threshed say 1%?

2 Procedure

2.1 Constraints from Old Experiments

F_UNCLE calculates how information from experimental measurements constrains uncertainty about models. We use a Mie Gruneisen form here, but rather than follow [5] and estimate a function for γ, we simply use a fixed value to get EOS functions from functions of one variable, namely $P_{S,CJ(\rho)}$. We use FLAG

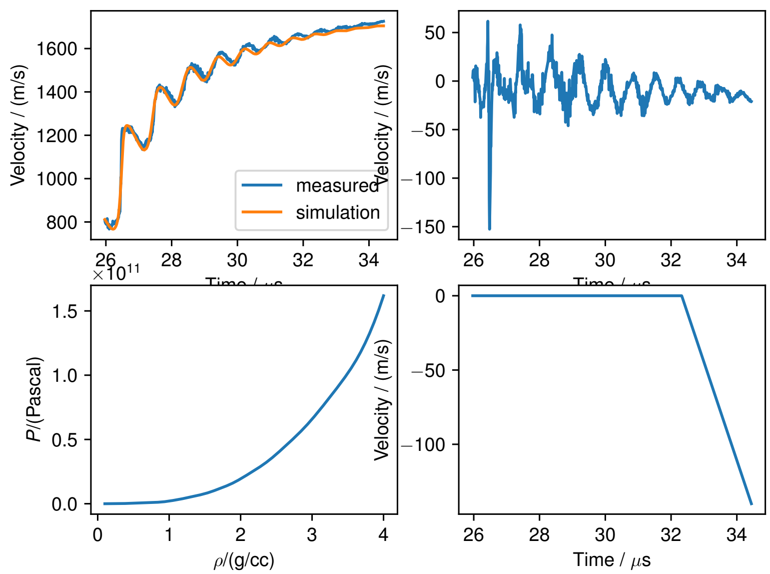

Figure 1: Plots of the the measured and simulated velocity (upper left), the difference ($\mathcal{E}$, upper right), the pressure on the CJ isentrope ($P_{S,CJ(\rho)}$, lower left), and the cost function (V_{cost}, lower right).

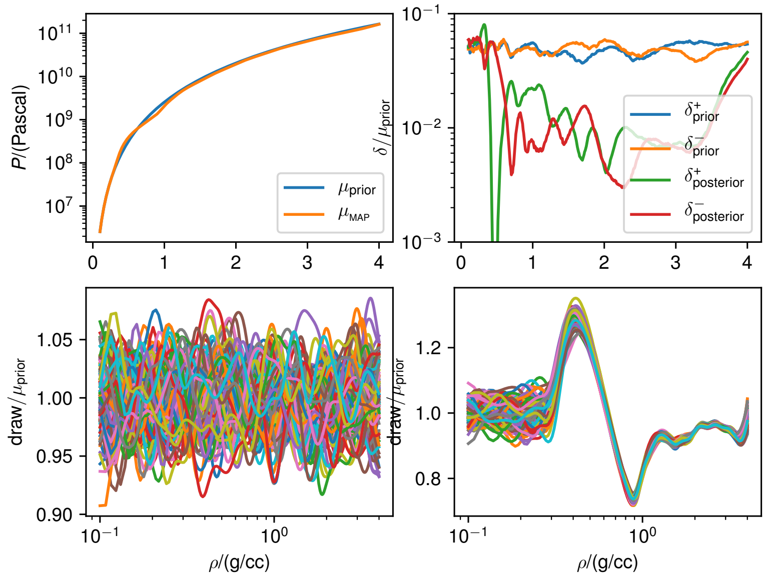

Figure 2: A comparison of the prior and a posteriori distributions of $P_{S,CJ(\rho)}$. The modes of the two distributions appear in the upper left plot. We used 100 random draws from the prior to make the plot in the lower left; plotting each sample divided by the mode. A similar plot of draws from the a posteriori distribution divided by the mode of the prior appears in the lower right. To make the plots of uncertainty bounds that appears in the upper right, we took 1000 random draws from each distribution and for each sampled value of ρ sorted the list of values of $P_{S,CJ(\rho)}(\rho)$ divided by the mean of the prior. Then we plotted the values at the 2.5% and 97.5% levels of that list.

simulations, Φ_{FLAG}, to map from pressure functions to deviation functions ϵ, writing

$$\epsilon(P)(t) = \Phi_{\text{FLAG}}(P)(t) - V_{\text{nominal}}(t). \tag{5}$$

We represent $P_{S,CJ(\rho)}$ as a vector, $\mathbf{a}$, of 55 basis function coefficients and then use probability distributions in $\mathbb{R}^{55}$ to characterizes uncertainty about $P_{S,CJ(\rho)}$. Figure 2 illustrates the how information from experiments constrains the uncertainty about $P_{S,CJ(\rho)}$.

2.2 Derivatives and Random Samples

With the map from coefficient vectors, $\mathbf{a}$, to functions, $P_{S,CJ(\rho)}$, we approximate the derivative of ϵ with respect to $P_{S,CJ(\rho)}$ by finite difference calculations:

$$D_i \approx \frac{\partial \epsilon}{\partial \mathbf{a}_i} = \frac{\partial \Phi_{\text{FLAG}}}{\partial \mathbf{a}_i}, \tag{6}$$

which requires 56 simulations.

F_UNCLE uses an un-normalized constrained Laplace approximation of the *a posteriori* probability density function of the vector $\mathbf{a}$, that defines a pressure function, P, ie,

$$\text{Prob}(\mathbf{a}) \propto e^{-\frac{1}{2}(\mathbf{a}-\mu_{\text{MAP}})^T \Sigma^{-1}(\mathbf{a}-\mu_{\text{MAP}})} \cdot I(\mathbf{a}) \equiv \mathcal{L}(\mathbf{a}) \tag{7}$$

where

$$I(\mathbf{a}) = \begin{cases} 1 & \text{if constraints are satisfied} \\ 0 & \text{otherwise} \end{cases} \tag{8}$$

We draw a set, $R = \{r_1, r_2, \cdots, r_N\}$, of random samples from the a posteriori distribution and calculate $\mathcal{L}(r)$ for each sample. To define a *plausible* vector of coefficients, we sort the random samples in order of the values $\mathcal{L}(r)$ and select a fraction F_{cutoff}. We define a cutoff value, $\mathcal{L}_{\text{cutoff}}$, with

$$\mathcal{L}_{\text{cutoff}} : \mathcal{L}(r) < \mathcal{L}_{\text{cutoff}} \text{ for exactly } F_{\text{cutoff}} \cdot N \text{ elements } r \in R. \tag{9}$$

Then we use $\mathcal{L}_{\text{cutoff}}$ to define a plausible coefficient vector, $\mathbf{a}$, as one that satisfies

$$\mathbf{a} \text{ is plausible } \iff \mathcal{L}(\mathbf{a}) \geq \mathcal{L}_{\text{cutoff}}. \tag{10}$$

Figure 3 illustrates the empirical cumulative distribution of values of $\mathcal{L}(r)$ for the values of $r \in R$. For this work the values are

$$\begin{aligned} N &= 1000 \\ F_{\text{cutoff}} &= 0.01 \\ \mathcal{L}_{\text{cutoff}} &= 1.246E - 13. \end{aligned}$$

2.3 Map from Measurements to Models with a Pseudo-Inverse

We seek an estimate of the pressure function that would produce the experimentally measured velocity, ie, $\operatorname{argmin}_P |\Phi_{\text{FLAG}}(P) - V_{\text{measured}}|$ which we approximate with the vector of coefficients

$$\mathbf{a}_1 = \mu_{\text{MAP}} + D^+ \mathcal{E}, \tag{11}$$

where D^+ is the Moore Penrose inverse

$$D^+ = \langle D, D \rangle^{-1} D, \tag{12}$$

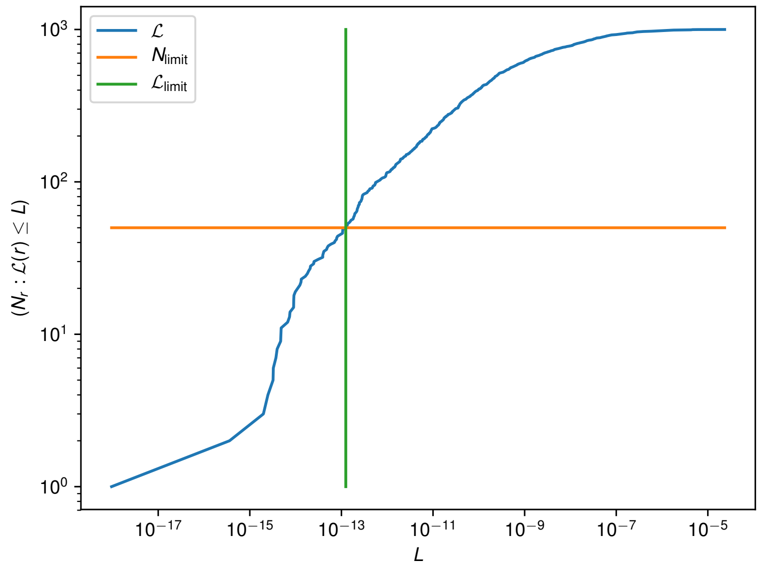

Figure 3: A plot of the empirical cumulative distribution of values of $\mathcal{L}(r)$. The horizontal line labeled N_{limit} illustrates a cutoff fraction $F_{\text{cutoff}} = 0.05$, and the vertical line labeled $\mathcal{L}_{\text{limit}}$ illustrates the corresponding value $\mathcal{L}_{\text{cutoff}} = 1.246E - 13$.

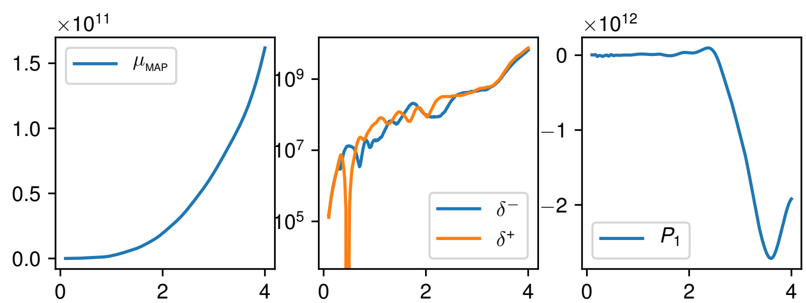

Figure 4: Pressure functions. The maximum of the a posteriori probability density appears on left. Bounds on plausible deviations appear in the center. And $\mathcal{P}_1$, estimated to explain the difference between the data and the simulation, appears on the right. Notice that $\mathcal{P}_1$ is not uniformly positive, monotonic, or convex.

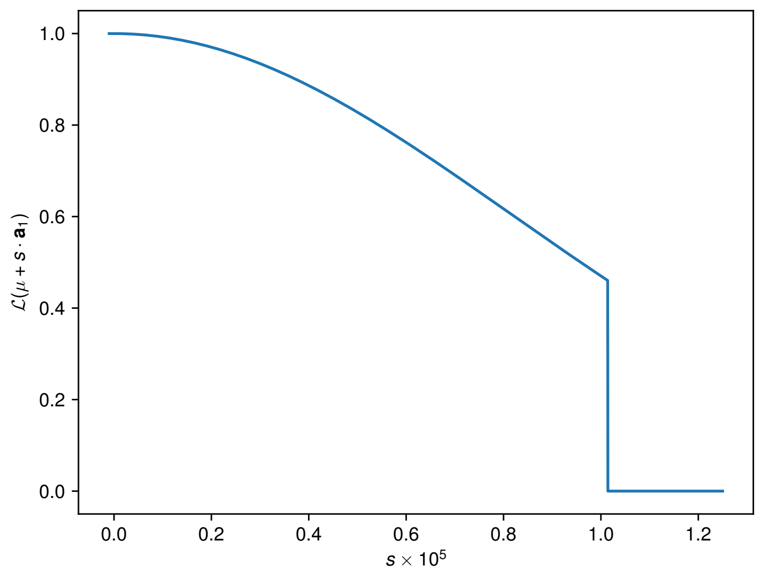

Figure 5: A plot of $\mathcal{L}(\mu_{\text{MAP}} + s \cdot \mathbf{a}_1)$, the Laplace function, vs s. Notice that the range of s is small and that the constraints exclude values $s > 1.014 \times 10^{-5}$, ie, any significant shift towards $\mathbf{a}_1$ violates the constraints. Thus the answer to the first question is "no"; the uncertainty in $P_{S,CJ(\rho)}$ is not large enough to permit the pressure function, $\mathcal{P}_1$, that would explain the velocity difference $\mathcal{E}$.

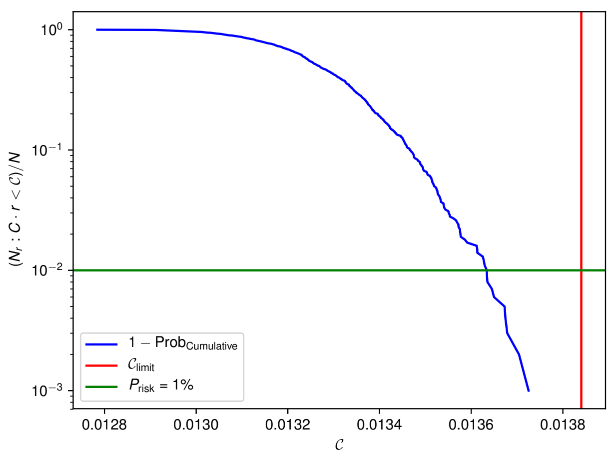

Figure 6: The complementary cumulative probability distribution of cost. The horizontal line illustrates the maximum acceptable risk, $P_{\text{risk}} = 0.01$, and the vertical line illustrates the maximum acceptable cost, $\mathcal{C}_{\text{limit}} = \langle V_{\text{cost}}, V_{\text{cost}} \rangle = 0.01384$. The lines intersect above the curve indicating that the answer to the second question is "yes"; the probability of $\mathcal{C} > \mathcal{C}_{\text{limit}}$ is less than 1%, ie, the risk is acceptable.

and D is defined in (6). We call the estimated pressure function $\mathcal{P}_1$. The plot that appears in Fig. 4 shows that $\mathcal{P}_1$ violates the positivity, monotonicity, and convexity constraints. Figure 5 illustrates the Laplace density along a line through $\mathbf{a} = \mu_{\text{MAP}}$ in the direction given by $\mathbf{a}_1$.

We also use the derivative to estimate the cost[1] of the pressure function corresponding to coefficients $\mathbf{a}$ with

$$\begin{aligned} C(\mathbf{a}) &= \mathcal{C}(D(\mathbf{a} - \mu_{\text{MAP}})) = \langle V_{\text{cost}}, D(\mathbf{a} - \mu_{\text{MAP}}) \rangle \\ &= \langle V_{\text{cost}}, D \rangle (\mathbf{a} - \mu_{\text{MAP}}). \end{aligned} \tag{13}$$

The distribution of costs corresponding to the random draws appears in Fig. 6.

3 Results and Conclusion

With these definitions, we more precisely state and answer the questions in Sect. 1 as follows:

Q1: Is the perturbation of the pressure corresponding to the vector of coefficients $\mathbf{a}_1$ plausible?

[1]We calculate the cost in terms of deviations from a nominal case. However, the experimental data indicates that our nominal model is flawed.

A1: No[2] Because $\mathcal{L}(\mathbf{a}_1) = 0$. It would only be plausible if $\mathcal{L}(\mathbf{a}_1) > \mathcal{L}_{\text{cutoff}} = 1.246E - 13$. Figure 5 illustrates the result.

Since no plausible change in the EOS model can explain the difference $\mathcal{E}$, we don't have a plausible model to use for answering **Q2**. To proceed, we suppose that we can identify and correct some other modeling error that explains the discrepancy $\mathcal{E}$.

Q2: For the cost functional defined in (4),

$$\mathcal{C}(\delta_\epsilon) \equiv \langle \delta_\epsilon, V_{\text{cost}} \rangle ,$$

we ask if P_{risk}, the probability of a cost higher than $\mathcal{C}_{\text{limit}}$, is less than 1%, ie,

$$P_{\text{risk}} \equiv \text{Prob}\left\{ \delta_\epsilon : \mathcal{C}(\delta_\epsilon) > \mathcal{C}_{\text{limit}} \right\} \leq 0.01? \tag{14}$$

A2: Yes, $F_{\text{cutoff}} < 0.01$, where F_{cutoff} is the fraction of elements, r, of R that satisfy

$$\begin{aligned} &\langle V_{\text{cost}}, D(r - \mu_{\text{MAP}}) \rangle > \mathcal{C}_{\text{limit}} \text{ or} \\ &\langle V_{\text{cost}}, D \rangle (r - \mu_{\text{MAP}}) > \mathcal{C}_{\text{limit}}. \end{aligned} \tag{15}$$

Figure 6 illustrates the result.

4 Notation

In Section 2 we introduced the following additional notation:

a: A vector of coefficients that are the degrees of freedom in a pressure function, $P_{S,CJ(\rho)}$.

$\mathbf{a}_1$**:** A linear estimate of the vector of coefficients that would resolve $\mathcal{E}$ the difference between the simulation and experiment. See (11).

D**:** The derivative of velocity with respect to degrees of freedom. See (6).

D^+**:** The pseudo-inverse of D. See (12).

F_{cutoff}**:** The fraction of draws deemed implausible. See (9).

I**:** The indicator function for the constraints. See (8).

$\mathcal{L}$**:** An un-normalized maximum a posteriori probability density function given by the Laplace approximation with constraints. See (7).

$\mathcal{L}_{\text{cutoff}}$**:** The smallest plausible value of $\mathcal{L}$. See (9) and (10).

[2] If rather than simply examining a line in the direction of $\mathbf{a}_1$ we searched in the direction of $\mathbf{a}_* \equiv \text{argmin}_{\mathbf{a}} |V_{\text{simulation}}(\mathbf{a}) - V_{\text{measured}}|$ subject to: $\mathcal{L}(\mathbf{a}_1) \geq \mathcal{L}_{\text{cutoff}}$, we might find a plausible pressure function that comes closer to explaining $\mathcal{E}$.

$\mathcal{P}_1$: The pressure function obtained from the degrees of freedom $\mathbf{a}_1$.

P_{risk}: The maximum acceptable probability of cost exceeding a threshold.

R: A set of vectors drawn randomly from $\mathcal{L}$.

r: An element of R.

γ: Gruneisen's gamma.

Φ_{FLAG}: The map from pressure functions to velocity functions implemented by the program named FLAG. See (5).

References

[1] Andrew M. Fraser and Stephen A. Andrews. Functional Uncertainty Constrained by Law and Experiment. In Sebastian Benthall and Scott Rostrup, editors, *Proceedings of the 15th Python in Science Conference*, pages 7 – 14, 2016.

[2] Stephen A. Andrews and Andrew M. Fraser. Estimating physics models and quantifying their uncertainty using optimization with a Bayesian objective function. *ASME Journal of Verification, Validation and Uncertainty Quantification*, 2019.

[3] Stephen A. Andrews, Andrew M. Fraser, Scott Jackson, and Eric Anderson. Understanding the uncertainty in an equation of state model for a high explosive obtained from heterogeneous data. In *Proceedings of the ASME 2019 V&V Symposium*, 2019.

[4] L. Hill. PBX9501 sandwich test data. Technical Report DX-2:02-119, Los Alamos National Laboratory, 2002.

[5] R. S. Hixson, M. S. Shaw, J. N. Fritz, J. E. Vorthman, and W. W. Anderson. Release isentropes of overdriven plastic-bonded explosive PBX9501. *Journal of Applied Physics*, 88(11):6287–6293, 2000.

[6] Steve J Pemberton, Tom D Sandoval, Tommy J Herrera, John A Echave, and Garry Maskaly. Test report for equation of state measurements of PBX9501. LA-UR 11-04999, Los Alamos National Laboratory, Los Alamos, NM, 2011.

[7] J. N. Fritz, R. S. Hixson, M. S. Shaw, C. E. Morris, and R. G. McQueen. Overdrivendetonation and soundspeed measurements in PBX9501 and the thermodynamic ChapmanJouguet pressure. *Journal of Applied Physics*, 80(11):6129–6141, 1996.

[8] Emily R. Pittman, Carl R. Hagelberg, Richard L. Gustavsen, and Tariq D. Aslam. Gas gun experiments and numerical simulations on the HMX based explosive PBX9501 in the overdriven regime. *AIP Conference Proceedings*, 1979(1):150032, 2018.